



UNIVERSITY OF LEEDS

This is a repository copy of *Hydraulic free-surface modelling with a novel validation approach*.

White Rose Research Online URL for this paper:
<http://eprints.whiterose.ac.uk/78803/>

Proceedings Paper:

Borman, DJ, Sleight, PA, Coughtrie, A et al. (1 more author) (2014) Hydraulic free-surface modelling with a novel validation approach. In: Proceedings of the 9th South African Conference on Computational and Applied Mechanics. 9th South African Conference on Computational and Applied Mechanics, 14-16 Jan 2014, Somerset West. . ISBN 978-0-620-58994-9

Reuse

Unless indicated otherwise, fulltext items are protected by copyright with all rights reserved. The copyright exception in section 29 of the Copyright, Designs and Patents Act 1988 allows the making of a single copy solely for the purpose of non-commercial research or private study within the limits of fair dealing. The publisher or other rights-holder may allow further reproduction and re-use of this version - refer to the White Rose Research Online record for this item. Where records identify the publisher as the copyright holder, users can verify any specific terms of use on the publisher's website.

Takedown

If you consider content in White Rose Research Online to be in breach of UK law, please notify us by emailing eprints@whiterose.ac.uk including the URL of the record and the reason for the withdrawal request.



eprints@whiterose.ac.uk
<https://eprints.whiterose.ac.uk/>

Hydraulic free-surface modelling with a novel validation approach

Duncan Borman^{1*}, Andy Sleigh¹, Andrew Coughtrie¹, Lucy Horton¹

¹ School of Civil Engineering, University of Leeds, Leeds, UK
d.j.borman@leeds.ac.uk

Abstract

This work shows that a three-dimensional transient two-phase RANS CFD-VOF model can be used to predict the position of waves and hydraulic jumps within a complex hydraulic flow environment as measured during a series of full-scale experiments. A novel application of LIDAR is used to provide detailed measurements of the position of the water free-surface location during the physical experiments. The test environment is a recreational white-water course that provides a means to vary the flow rates of water and restrict the flow easily as required. Obstructions are added to the channel to create hydraulic jumps and other specific flow features. The influence of these obstructions on the flow has been analysed for size, velocity and position. The results of the study demonstrate that, although computationally intensive, the free-surface CFD approach can reliably predict a range of complex hydraulic flow features in medium/large-scale open channel flow conditions. In order to reliably capture the full three-dimensional characteristics of the water free-surface a high resolution mesh (greater than 2.5 million cells) with time-steps in the order of milliseconds is necessary (Simulations presented here represent between 30 and 60 seconds of real-time).

Keywords: CFD, modelling, VOF, free-surface, hydraulic jump, white-water, LIDAR, TLS, waves, kayaking

INTRODUCTION

Hydraulic modelling can support the design of water features where there is a need to understand the shape and location of a water surface alongside a three dimensional velocity distribution and related flow phenomena. Examples include river management interventions (such as weirs and spillways) as well as the design of flow characteristics in recreational white-water courses. Commercial recreational white-water sports can be categorized as rafting, canoeing and kayaking: subgroups of white-water kayaking are river running and play-boating. A further subcategory of river running is slalom kayaking, in which competitors race to navigate their way downstream whilst passing through a number of gates –it is an event in the Olympic Games, first introduced in 1972. There are currently over 40 slalom courses in the UK alone. Play-boating involves performing technical moves or acrobatic tricks on river (or channel flow) features, usually standing waves, hydraulic jumps and ‘holes’, so they will often remain on the same section of the water for a period of time. Often these two types are combined and kayakers will stop to ‘play’ at various locations during their descent down the river. These white-water sports can either be undertaken on rivers or man-made courses (or a hybrid combination of the two). White-water courses, both natural and man-made, are formed by water flowing through a channel of changing cross section, typically over submerged obstacles; that induce hydraulic jumps and recirculating flows. Standing waves are a key component of a course and act as features for kayakers to traverse a flow or for use in performing manoeuvres and stunts (e.g. surfing a wave). Standing waves can be smooth or breaking; breaking waves are typically spilling or plunging in character. These occur when the critical amplitude and velocity of the wave crest are exceeded and the wave overturns, creating turbulence and white-water. Breaking waves occur most commonly in shallower water and are desirable for surfing. Budwig et al. [1] explain that stable standing waves are favourable for kayakers with desirable features including a large wave height, a thin layer of reverse flow at the surface (called the surface roller) and downstream submerged currents. This submerged current is desirable as a safety feature as it ensures that swimmers will be swept downstream rather than being caught up in the wave. Figure 1 shows a schematic of a desirable standing wave. One of the problems with natural white-water rivers is that they are weather dependent so if the discharge is not high enough, white-water

activities will not be possible; on the other hand if the discharge is too great they could pose an unacceptable risk to recreationalists. It is therefore useful to be able to design and have some control over the types of waves and features to allow participants of all abilities to enjoy the sport, as such artificial white-water courses are becoming increasingly widespread.

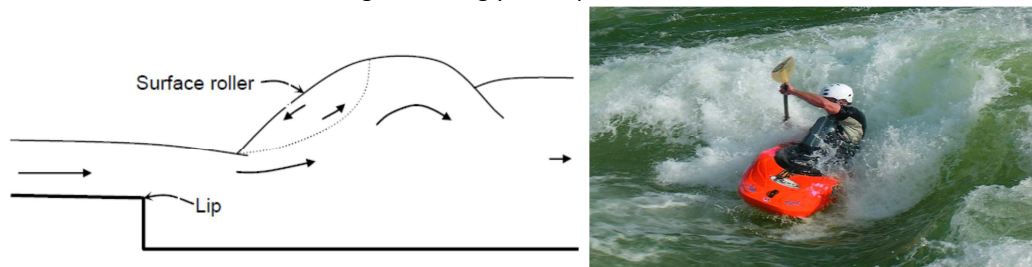


Figure 1 Standing wave (left) schematic of a standing wave at an abrupt drop (taken from Budwig et al [1], and (right) kayaker surfing a 'high-quality' standing wave

The location of standing jumps can typically result in 'playable' stationary waves. As such, being able to reliably predict the location and character of the hydraulic jump is important in the design of a course. Typically a hydraulic jump forms when high velocity flow discharges into a channel or structure that sustains a lower velocity flow. It is characterised by flow transitioning from supercritical to subcritical flow (by definition a Froude number less than 1 means the flow is subcritical and greater than 1 the flow is supercritical). When the change from supercritical to subcritical flow occurs the transition is sudden and causes an abrupt discontinuity of the water surface (and an associated loss in energy) which can result in a stationary wave. Hydraulic jumps occur frequently where a steep gradient bed suddenly flattens out into slow moving volume of water as exploited in many white-water courses. Establishing the Froude number and thus the location (and character) of the hydraulic jump for a constant section channel is relatively straightforward [2, 3]; however for the changing section of a real channel it is non-trivial. Hydraulic jumps can be undular, breaking or somewhere in between. The classification is based on the Froude number and the amount of energy lost and characterised based on the shape and height that the flow takes; a good description is provided by Inamdar [4]. The most advantageous type, when considering white-water course features, is a stationary jump as this remains fixed in one place and dissipates energy causing high turbulence (as white water) and the desired character of the white-water stationary wave. In addition strings of undular jumps are also desirable to create a rippled white-water effect for kayakers. Jumps with higher Froude numbers tend to have surface rollers that are extremely desirable to white-water recreationalists.

Murzyn and Chanson [5] highlight that there is still relatively little information available on the two-phase interaction and roller properties of turbulent hydraulic jumps. Furthermore, Rostami et al. [6] report that there are limited studies conducted around the detailed behaviour of hydraulic jumps with particularly few on the undular type where there can be several transitions from supercritical to subcritical state. The experimental studies conducted by Murzyn and Chanson [5] provide useful insight into jumps with high Froude numbers ($5 < Fr < 8.5$) and Reynolds numbers between 38000 and 62000. Rostami et al. [6, 7] performed numerical simulations on hydraulic jumps of the undular type on gravelled and smooth beds respectively, of character close to that found on white-water courses, using the CFD-VOF approach. Lin et al. [8] again used CFD (VOF approach) for predicting hydraulic jumps on the Calgary Bow River in order to create recreational opportunities. They indicated that the models correctly predicted the hydraulic jump position suggesting that it is a viable tool in the design of hydraulic features. Currently the approach for designing and testing white-water courses prior to prototype construction is to use a combination of Froude scale hydraulic model (typically 1:10 scale), 2D shallow-water equation based models, prior experience and trial and error [9]. By creating a physical scale model of a channel, if the Froude number in both the model and the physical channel are matched then the characteristics of the flow, such as velocity, wave height and fluid depth, will be comparable. However, these Froude-scale physical models are expensive (typically in excess of £200,000). Furthermore, due to their size they are typically disassembled shortly after

construction rendering them unavailable for supporting refinement and modification of constructed courses in future years.

There is potential for increased application of numerical modelling where detailed flow information is required for real-world environments. Recent developments in free-surface CFD approaches alongside wider accessibility to high-performance computing facilities have meant that simulations that would have been unfeasible even five years ago are now a realistic prospect for many industrial hydraulic applications [8, 10]. In recent years CFD has become an increasingly popular tool for attempting to model such fluid flows with the Volume of Fluids (VOF) approach being widely used to simulate free-surface problems. It has been used for predicting the formation of stationary waves where the method performs generally well for a range of flows. However, there have been only limited studies undertaken where the VOF model has been evaluated and validated against real environmental flows. An advantage of the VOF method is that it only requires one value for the free surface to be stored in each cell. There are a variety of formulations for the VOF model and a wide range of studies have been conducted using the method (in various formulations) to track an interface between water and air. For example Gopala and van Wachem [11] compared different formulations of VOF, namely: flux-correlated transport, Lagrangian piecewise linear interface calculation (L-PLIC) and a compressive interface capturing scheme for arbitrary meshes. They found that the latter approach produced the most accurate results when compared with experimental data, whilst also maintaining a sharp interface. The VOF method was combined with the shallow water equations in a study by Ozmen-Cagatay and Kocaman [12] to simulate a dam-break flow reliably, but with small discrepancies in predictions for the depth of the water. Kositgittiwong et al. [13] used the VOF method to investigate the effects of turbulence and Lin et al. [8] used the VOF method as a way of assessing where a hydraulic jump would form in a proposed recreational water development. One of the main disadvantages of the VOF method is that the interface curvature must be approximated since a direct calculation is not possible due to the gradient of the VOF being discontinuous. To help overcome this problem the Level Set (LS) method was developed for multiphase flow by Sussman et al. [14]. Combining the advantages of the VOF method and the level set method, Sussman and Puckett [15] developed a coupled level set/volume of fluid (CLSVOF) method. Wilson et al. [16] used this combined CLSVOF method successfully in their study to predict breaking bow waves. When using the VOF method, the volume fraction equation transport equation can be solved implicitly or explicitly. The explicit method when implemented with a piecewise linear interface calculation (PLIC) is generally considered to be the most reliable for retrieving time-accurate transient free-surface behaviour [17]. When this method is used, the need for the combined level set and VOF method is reduced as the free surface is modelled in a piecewise manner and the curvature problem is removed.

For turbulent flows, the Reynolds Averaged Navier Stokes (RANS) approach (which incorporates a turbulence model to close the Reynolds stress terms) is a common and robust approach. In terms of selecting a suitable turbulence model, studies using VOF have found that the $k - \epsilon$ RNG model performs generally well. Bakhtyar et al. [18] compared the standard $k - \epsilon$, the $k - \epsilon$ RNG and the $k - \omega$ model for flow in surf and swash zones for waves close to a shoreline. They found that the $k - \epsilon$ RNG model yielded the most accurate predictions, the standard model performed satisfactorily and the $k - \omega$ model predicted the breaking points of the waves early. Further examples of studies that have used the standard or RNG $k - \epsilon$ models include: Bradford [19], who found that both models predicted waves in the surf zone well with the RNG model having an advantage prior to breaking; Hieu et al. [20] simulated breaking waves using the VOF method and found predictions accurate within the surf zone but under predicted the wave height at breaking point; Xie [21, 22] modelled breaking waves using the standard and $k - \epsilon$ RNG models and the results indicated that the RNG performed better in the surf zone but predicted lower turbulence intensities in the outer zone. The $k - \epsilon$ RNG model was also used in studies by Oertel et al. [23] who reported its accuracy for prediction of free surface flows.

In this work the VOF-PLIC approach will be implemented and evaluated as a method to reliably predict the three-dimensional free-surface location of real flows as found in a recreational white-water course. The model will be used to simulate the position of the hydraulic jump and associated stationary wave through a real channel. Experiments, conducted for a range of flow rates and geometries, will be used to provide

validation data. A novel application of a Terrestrial LIDAR System (TLS) provides measurements of the position of the water free-surface location.

EXPERIMENTAL AND NUMERICAL MODEL

Physical Model

The test environment is a recreational white-water course that provides a means to vary the flow rates of water and restrict the flow as and when required. The physical channel is approximately 65m in length (from 'inlet' gate to downstream 'outlet' weir) with the channel bed having a fall of 3.1m over this length. The width of the channel ranges from approximately 4.5m to 23m. The flow rate of water into the channel is controlled by a movable gate that can be lowered incrementally to release water from the upstream channel. A StreamPro acoustic doppler current profiler (ADCP) is used to measure velocity profiles across the channel for each experimental trial, which in turn are used to calculate the flow rate for each experiment. A TLS (Topcon GLS 1500) was used to scan the empty channel bed and geometry and to record returns from the white-water. TLS is not traditionally used to measure the surface of water, as there is no return; however the researchers have previously found that the broken water surface of white-water provides enough signal to capture the detail of a stationary wave and water surface in key locations [24].

Figure 2a provides an overview of the experimental channel with key features such as the location of the inlet gate and downstream weir identified. The weir height at the exit of the channel was initially set to 0.25m in height and in later studies was increased to 0.5m. Figure 2b shows zoom view of the channel bed where the hydraulic jump is observed to form and where 'obstacle blocks' have been inserted onto the channel floor for the latter experiments.

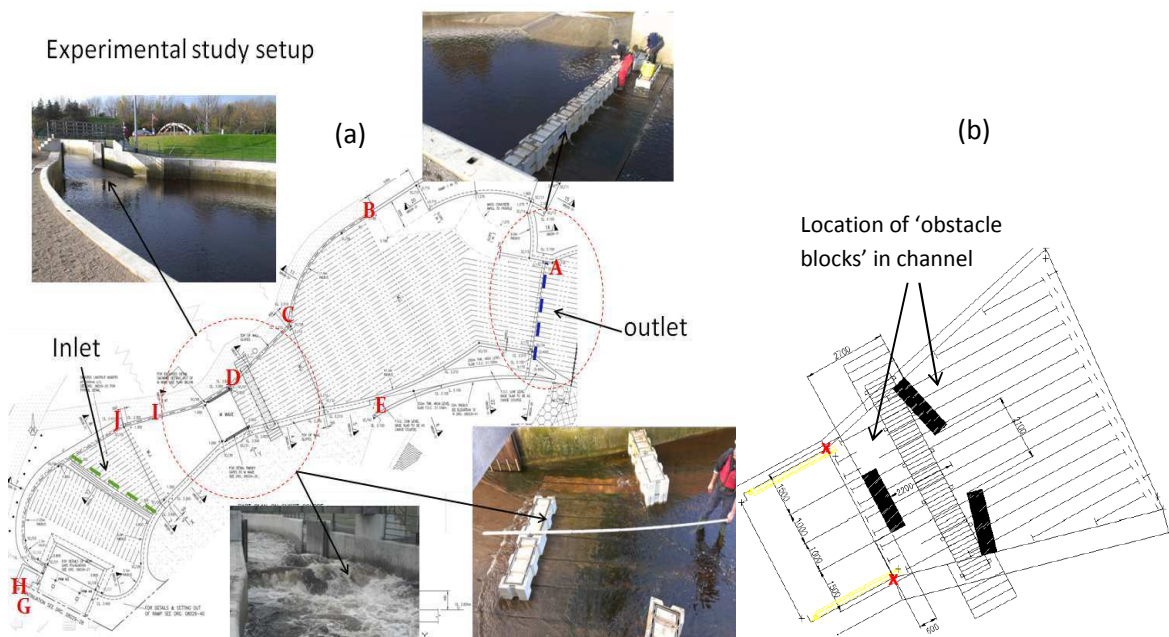


Figure 2 (a) Schematic of the full course showing water inlet gate and outlet weir locations, (b) expanded view of the region where hydraulic jump forms and where additional 'obstacle blocks' added.

Table 1 outlines detail of seven experimental trials conducted. Trials 1-4 have no additional obstacle blocks inserted into the channel floor and involve varying the flow rate and downstream weir height. Trials 5 and 6 insert obstacle blocks into the channel as seen in the location set out in Figure 2b, for high and low discharge rates. Figure 7 and 8 are the same experiment, but with an increased height of block (on the same footprint). In each experiment a high (H) and low (L) flow was used; the absolute flow rate varied due to conditions over the 10 hour duration of the trial period. Low flows are between $2.1\text{-}3.1\text{ m}^3\text{ s}^{-1}$ and high flow above $5.0\text{ m}^3\text{ s}^{-1}$. The block arrangement 'B1' can be observed in figure 2.

Table 1 Overview of experimental trials

Trial number	1	2	3	4	5	6	7	8
Outlet weir height (m)	0.25	0.25	0.25	0.5	0.5	0.5	0.5	0.5
Flow rate (H/L)	VH	H	L	L	L	H	L	H
Flow rate (m^3s^{-1})	8.3	6.9	2.9	3.1	2.1	5.5	2.3	5.5
Inserted block formation*	B0	B0	B0	B0	B1	B1	B2	B2

*B0 = no 'obstacle blocks' in channel

B1 = side blocks: 2 high 2 wide, central blocks base: 1 high, 2wide

B2 = side blocks: 3 high 2 wide, central blocks base: 1 high, 2wide, central blocks 2nd layer: 1 high

An obstacle block dimensions are: 0.25m x 0.5m x 1.0m

Numerical Model

The solver Ansys Fluent 13.0 was selected for the numerical modelling as it provides robust and convenient implementation of the VOF-PLIC method. A RANS CFD approach is implemented in the work which incorporates an explicit VOF model to predict the transient free-surface behaviour of white-water. A description of the VOF-PLIC model is found in [17]. An initial pilot study is used to assess the approach including mesh requirements and sensitivity to turbulence model as required for the main study. In the main numerical study 3D numerical simulations are run for each of the experimental trials outlined in Table1. For the each case the boundary conditions used are based on the experiments with the water having a mass flow rate equated from the volume flow rate. Furthermore in each case the CFD is run transiently allowing the water to fill the channel and is left to run until a steady flow is reached.

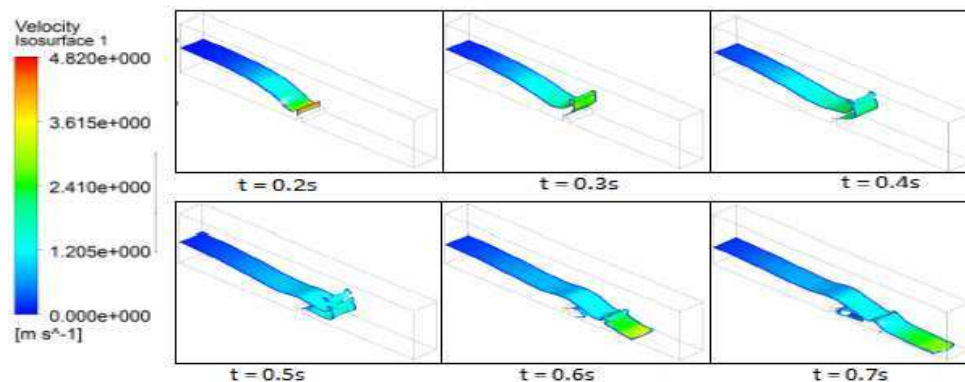
Table 2 Overview of boundary conditions for main CFD study

Boundary	Water phase	Air phase
Inlet water	Mass flow rate (derived from flow rate in table 1)	n/a
Outlet	Atmospheric pressure	Atmospheric pressure
Walls	No slip condition	No slip condition
Atmosphere	n/a	Atmospheric pressure

RESULTS AND DISCUSSION

Pilot study

The pilot modelling study carried out on a simplified geometry is used to evaluate the approach, assess the sensitivity of predictions to turbulence modelling and investigate mesh requirements. This study was performed on a simple 3D geometry in a 2m x 0.5m x 0.2m rectangular duct with a small 0.1m high block cut out of the channel bed. A dam break situation was simulated similar to that of Pracht [25] with a block of water measuring 0.4m x 0.4m x 0.2m initially patched at one end of the channel. The simulations were run transiently using the VOF-PLIC with the $k - \epsilon$ RNG turbulence model and a time-step of 0.005 seconds. All boundaries are taken as zero velocity no-slip walls except for the side walls where a zero shear, slip condition was applied. A sharp air-water interface is obtained and the location of this over time is shown in figure 3 for the first 0.7 seconds.

**Figure 3** Predictions of free-surface location over time for the pilot study (coloured by velocity magnitude)

Mesh independence was investigated with three mesh sizes of increasing size used- 25,000, 100,000, 225,000 elements (it should be noted that for the finest mesh, a time step of 0.0025 seconds was required to keep the global courant number from becoming too large and the solution diverging). The free-surface along the centre profile is shown in figure 4. The finer of the 2 meshes are consistent for key aspects of the flow that is useful for understanding the mesh requirements for the full-scale study. Extrapolating from this study it is anticipated that for the full-scale study mesh elements of between 10-100mm in length will be required. In the main CFD study the base mesh used has 2.4 million elements with 55 elements in the vertical direction (z), 100 across the width (y) and 440 in the stream-wise direction (x). The obstacle blocks are removed by extracting whole cells from the domain mesh. As an example of the mesh size, in the region close to the obstacle blocks, the cells are approximately 60mm x 40mm x 40mm.

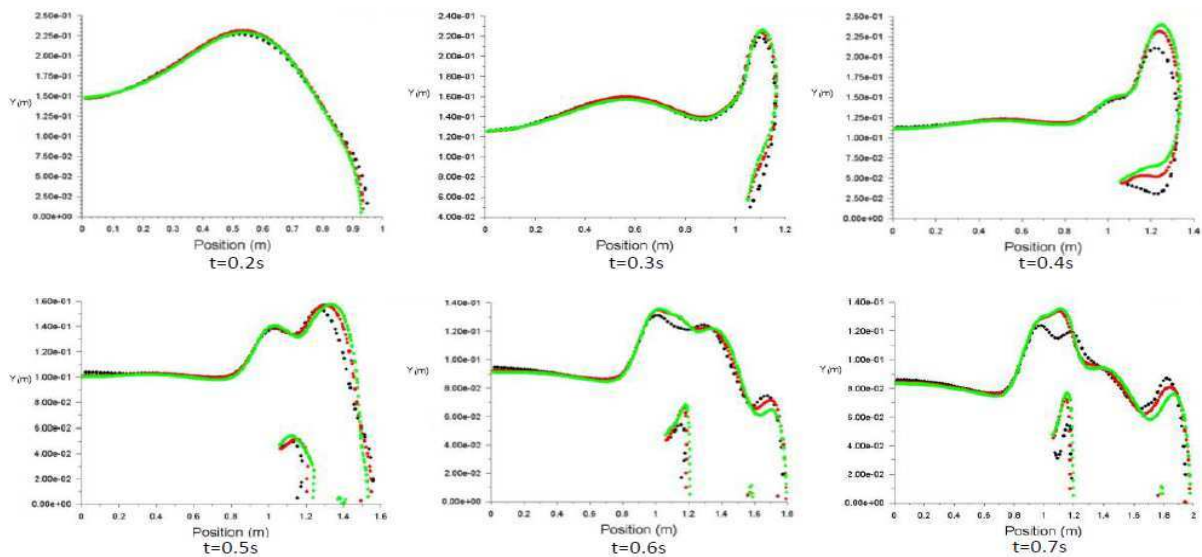


Figure 4 Free-surface predictions over time for the pilot study for increasing mesh sizes (25,000=blue, 100,000=red, 225,000=green)

Figure 5 shows the same test simulations for the 100,000 size mesh and includes results for two further turbulence models. The blue data points represent the $k - \epsilon$ RNG, the red the standard $k - \epsilon$ and green the $k - \omega$ SST model. In general, the simulations are comparable with the $k - \epsilon$ RNG and $k - \omega$ SST models predicting the location of the free-surface generally more in line with one another. Based on these tests and the previous literature the $k - \epsilon$ RNG model will be used to model turbulence in the full-scale study.

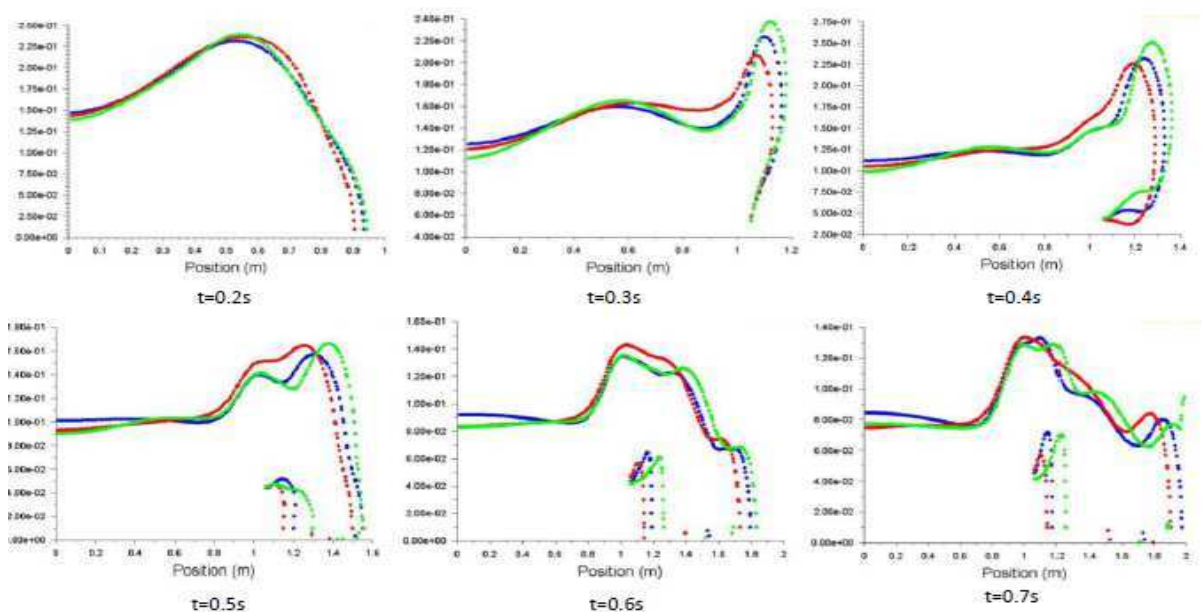


Figure 5 Free-surface prediction over time for pilot study for 3 turbulence models (blue= $k - \epsilon$ RNG, red=standard $k - \epsilon$, green= $k - \omega$ SST)

Without Obstacles

Before considering the examples with obstacles inserted in the channel, trials 1-4 were undertaken to investigate the location and shape of the stationary wave forming for different flow rates and downstream weir heights. The mesh used is a regular hexahedral structured mesh throughout. Figure 6a shows the point cloud data for experimental trial 1. Both the channel and stationary wave are captured clearly using the TLS. Figure 6b shows the side profile of the point clouds for trials 1-4. As expected the higher flow rates create a larger and more energetic hydraulic jump; however, the location at which the jump occurs is similar for each of the discharge rates. In the case of trial 3 and 4, where the low discharge rate is used, the impact of increasing the downstream weir height is observed to move the location of the hydraulic jump upstream (as expected due to the higher water level it induces).

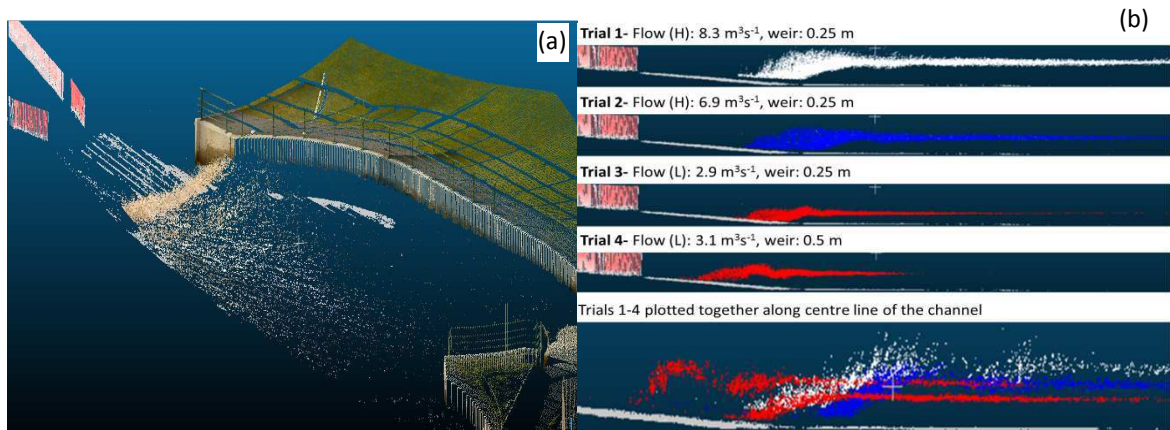


Figure 6 TLS point cloud of the channel (a) 3D view showing reflected white-water for trial 1, (b) horizontal plane view of white-water surface for Trials 1-4

Figure 7a and 7b show the process of overlaying the three-dimensional point cloud for the TLS measured white-water surface onto the the free-surface prediction for the VOF simulation. The case shown is for the low discharge rate and low downstream weir height (trial 3). To aid analysis the point clouds can be separated into thin parallel strips. It can be observed that the model predicts the hydraulic jump well in terms of both position and height. This is further supported by the photograph shown in figure 7c which shows the forming hydraulic jump and provides a good visual comparison with the CFD and measured TLS data. A similar level of good agreement is also found for trials 3 and 4.

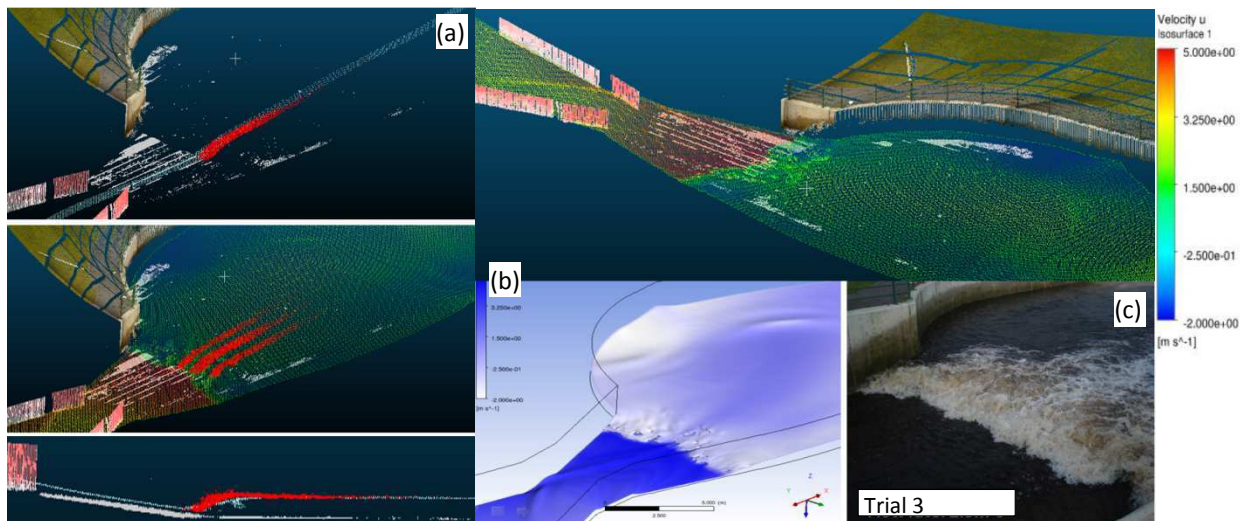


Figure 7 Predictions for Trial 3 (a) TLS point cloud and CFD free-surface prediction shown together (b) The CFD prediction (c) a photograph of the hydraulic jump/stationary wave

Obstacle blocks inserted prior to the hydraulic jump

The two different obstacle block arrangements were simulated at both high and low discharge rates. Figure 8 shows the visualisations of the free-surface predictions (coloured by stream-wise velocity) and associated

photographs of the experiments in trials 7 and 8. Comparing figures 8a and 8b (trial 8) the free-surface shape and location can be seen to be qualitatively in good agreement with the flow observed in the photograph. Key flow features are predicted well -with for example the water level over the blocks correctly simulated and the undular shape of the flow, and location of the rollers clearly identified. Furthermore, the location of the hydraulic jump after the obstructions is correctly predicted in terms of position, shape and height. A similar good result is observed for trial 7, where for the lower discharge rate, there is both observed and simulated a reduction in flow over the side blocks compared with the high discharge case (figure 8c and 8d). Water levels are observed to be comparable and both the breaking wave that forms between the blocks and the shape and location of hydraulic jump are correct in the simulations. A similar level of good qualitative agreement for the free-surface location is also observed for Trials 5 and 6. Figure 9a shows the predicted free-surface location on a vertical plane down the centre of the channel for each of trials 5-8. Figure 9b shows the same predictions in the region around the obstacles, overlaid with the TLS measurements of the white-water surface. From this comparison it can be observed that although the main flow features are predicted well (for example the water levels, the slope of the water surface) the location of other features appears to be predicted too early along this central plane (for example the position of the wave undulation in trail 6). However, it should be noted that these flows have a small degree of localised transient behaviour. This is observed both in the transient CFD runs and physical observations. As such, the CFD, TLS and photographic result are each a ‘snap-shot’ that are not exactly synchronised. This in part could be a cause of some small localised differences between the model and measurements. This will be investigated in more detail in the next steps of the work.

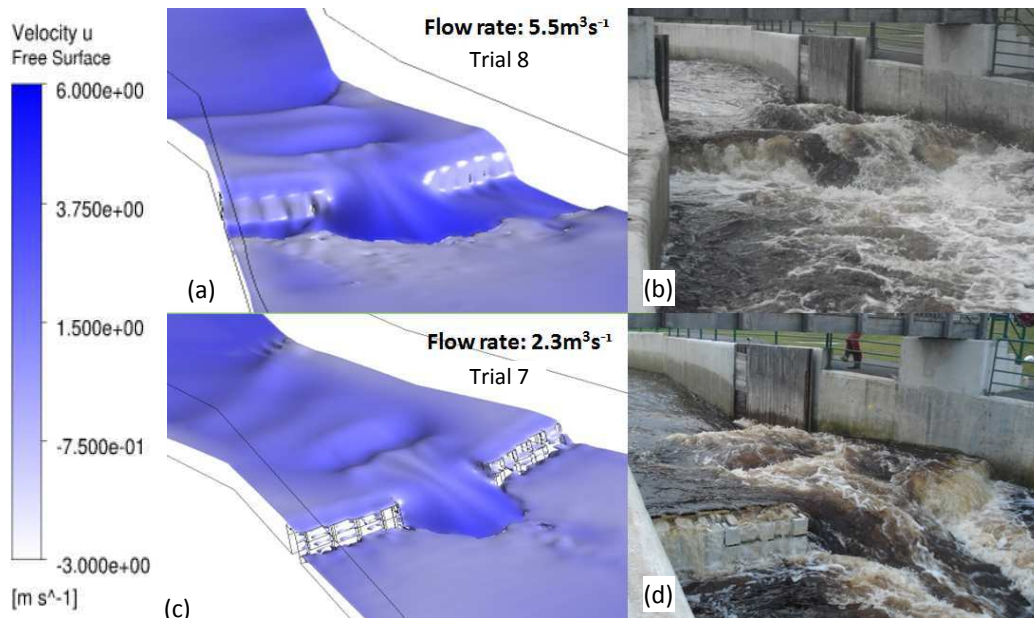


Figure 8 CFD free-surface predictions coloured by stream-wise velocity and associated photograph for Trial 8 (a), (b), respectively and for Trial 7 (c), (d), respectively.

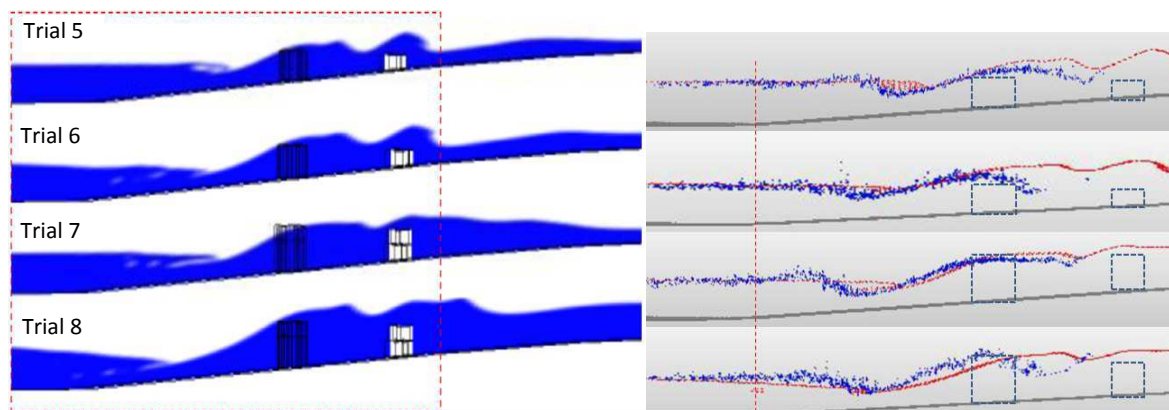


Figure 9 Free-surface location at the centre of channel for trials 5-8 (a) CFD free-surface predictions (b) CFD predictions and experimental results in region around the obstacle blocks (red=CFD, blue=TLS).

CONCLUSION

The results of the study demonstrate that, although computationally intensive, the free-surface CFD approach evaluated can reliably predict the key features of complex hydraulic behaviour in medium/large-scale open channel flow conditions. In order to reliably capture the full three-dimensional characteristics of the water free-surface a high resolution mesh (2.5 million+ cells) with time-steps in order of milliseconds is necessary (running for around 30-60 seconds of real-time simulation). There are numerous potential industrial application areas where this approach can be exploited. These include applications in the design of 'play features' at recreational white-water courses (such as Lee-Valley Olympic White-Water Centre) as well as providing a meaningful tool for design of river management systems.

REFERENCES

1. BUDWIG, R., MCLAUGHLIN, R. E., CLAYTON, S., SWEET, S. & GOODWIN, P. , *Physical modeling of wave generation for the Boise River Recreation Park*, *Proceedings of the International Conference of Science and Information Technologies for Sustainable Management of Aquatic Ecosystems* 2009: Concepción, Chile.
2. Gharangik, A.a.C., M., *Numerical Simulation of Hydraulic Jump*. *Journal of Hydraulic Engineering*, 1991. **117**(9): p. 1195-1211.
3. Chow, V.T., *Open-Channel Hydraulics*. 1959: McGraw-Hill.
4. Inamdar, S. *Hydraulic jump and weir flow [Online]*. . 2010 [cited 2013 04/12/2013]; Available from: http://udel.edu/~inamdar/EGTE215/Jump_weirs.pdf.
5. MURZYN, F., CHANSON, H. , *Two-phase flow measurements in turbulent hydraulic jumps*. *Chemical Engineering Research and Design*, 2009. **87**: p. 789-797.
6. ROSTAMI, F., YAZDI, S. R. S., SAID, M. A. M., SHAHROKHI, M. , *Numerical simulation of undular jumps on graveled bed using volume of fluid method*. *Water Science and Technology*, 2012. **66**: p. 909-917.
7. ROSTAMI, F., SHAHROKHI, M., SAOD, M. A. M., YAZDI, S. R. S. , *Numerical simulation of undular hydraulic jump on smooth bed using volume of fluid method*. *Applied Mathematical Modelling*, 2013. **37**: p. 1514-1522.
8. LIN, F., SHEPHERD, D., SLACK, C., SHIPLEY, S. & NILSON, A. *Use of CFD Modeling for Creating Recreational Opportunities At the Calgary Bow River Weir*. *World Environmental and Water Resources Congress*. 2008. Ahupua'a.
9. SHIPLEY, S., LAIRD, A., VANDERPOL, M., PHEIL, C. , *The use of computer and physical modeling to evaluate and redesign a whitewater park.*, in *Whitewater Courses & Parks 2010* 2010: Colorado, USA.
10. Kim S., H.-J.L., An, S., *Improvement of hydraulic stability for spillway using CFD model*. *International Journal of the Physical Sciences*, 2010. **5**(6): p. 774-780.
11. GOPALA, V.R.V.W., B. G. M., *Volume of fluid methods for immiscible-fluid and free-surface flows*. *Chemical Engineering Journal*, 2008. **141**(1–3): p. 204-221.
12. OZMEN-CAGATAY, H., KOCAMAN, S. , *DAM-BREAK FLOW IN THE PRESENCE OF OBSTACLE: EXPERIMENT AND CFD SIMULATION*. *Engineering Applications of Computational Fluid Mechanics*, 2011. **5**: p. 541-552.
13. KOSITGITTIWONG, D., CHINNARASRI, C. & JULIEN, P. Y. , *Numerical simulation of flow velocity profiles along a stepped spillway*. *Journal of Process Mechanical Engineering*, 2013.
14. SUSSMAN, M., SMERKA, P. & OSHER, S., *A LEVEL SET APPROACH FOR COMPUTING SOLUTIONS TO INCOMPRESSIBLE 2-PHASE FLOW*. *Journal of Computational Physics*, 1994. **17**: p. 132-159.
15. SUSSMAN, M.P., E. G. , *A coupled level set and volume-of-fluid method for computing 3D and axisymmetric incompressible two-phase flows*. *Journal of Computational Physics*, 2000. **162**: p. 301-337.
16. WILSON, R.V., CARRICA, P. M. & STERN, F. , *Simulation of ship breaking bow waves and induced vortices and scars*. *International Journal for Numerical Methods in Fluids*, 2006. **54**: p. 419-451.
17. Youngs, D.L., *Time-dependent multi-material flow with large fluid distortion*. *Numerical methods for fluid dynamics* 1982 **24**: p. 273-285.
18. BAKHTYAR, R., RAZMI, A. M., BARRY, D. A., YEGANEH-BAKHTIARY, A. & ZOU, Q. P., *Air-water two-phase flow modeling of turbulent surf and swash zone wave motions*. *Advances in Water Resources*, 2010. **33**: p. 1560-1574.
19. BRADFORD, S.F., *Numerical simulation of surf zone dynamics*. *Journal of Waterway Port Coastal and Ocean Engineering-Asce*, 2000. **126**: p. 1-13.
20. HIEU, P.D., KATSUTOHI, T., CA, V. T., *Numerical simulation of breaking waves using a two-phase flow model*. *Applied Mathematical Modelling*, 2004. **28**: p. 983-1005.
21. XIE, Z., *Two-phase flow modelling of spilling and plunging breaking waves*. *Applied Mathematical Modelling*, 2013. **37**: p. 3698-3713.
22. XIE, Z.H., *Numerical study of breaking waves by a two-phase flow model*. *International Journal for Numerical Methods in Fluids*, 2012. **70**: p. 246-268.
23. OERTEL, M., MONKEMOLLER, J., SCHLENKHOFF, A. , *Artificial stationary breaking surf waves in a physical and numerical model*. *Journal of Hydraulic Research*, 2012. **50**: p. 338-343.
24. BORMAN D.J., S.P.A., EVANS A., *Scanning for Hydraulic modelling*, in *Scanning for Hydraulic modelling, SPAR Europe 3D Imaging and Imaging Conference/European Mapping Forum*, SPAR: Amsterdam.
25. PRACT, W.E., *CALCULATING THREE-DIMENSIONAL FLUID FLOWS AT ALL SPEEDS WITH AN EULERIAN-LAGRANGIAN COMPUTING MESH*. . *Journal of Computational Physics*, 1975. **17**: p. 132-159.

